This Publication Is Distributed To Members Only

Harmonics and Transients Tech Notes

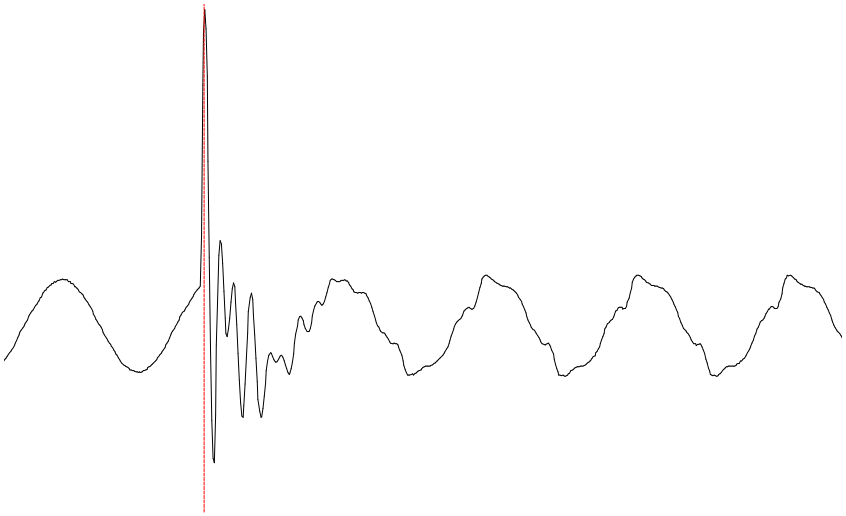

Issue # 97-1 ***April 1997*** ***Editor: Kathryn Nix***

Project Manager: Huyen Nguyen

In this issue:

Letter from the Project Manager

Dear PATH Members:

We have added a new member to the PATH Users Group staff here at Electrotek. Kathryn Nix is our new PATH Users Group Coordinator. Kathryn has already assisted many of you with questions or problems, so you know first hand what an asset Kathryn is going to be to PATH. Kathryn is rapidly learning the PATH ropes, so those of you who have not met Kathryn yet, please do not hesitate to contact her with your questions or concerns. We all need to give Kathryn a warm welcome into our PATH group.

One way you can welcome Kathryn is to send her your articles for publication in *Tech Notes*. I know she will look forward to receiving articles from any of you but especially the from the university members. As I stated in the previous *Tech Notes*, the article does not have to be about a final product. It can be a synopsis of the project during its planning or developing stages. The main idea is to provide other members of the group with an up-to-date information source on what takes place in today's power system engineering world.

One last thing, our annual PATH Users Group Meeting will be held October 20-22. We will be sending you a brochure with all the important details, but please mark your calendars and make plans to attend this year's meeting.

Sincerely,

Huyen V. Nguyen
huyen@electrotek.com

For more information concerning the newsletter or to submit a contribution please contact

Kathryn Nix
Electrotek Concepts, Inc.
408 North Cedar Bluff Road, Suite 500
Knoxville, Tennessee 37923
Phone: (423) 470-9222 x118
FAX: (423) 470-9223
e-mail: kathryn@electrotek.com

This paper was presented at the IEEE/IBCPS Conference, San Antonio, Texas
May 1995

Transient Effects of PWM Drives on Induction Motors

Christopher J. Melhorn
Electrotek Concepts, Inc.
Knoxville, Tennessee 37932

Le Tang
ABB Power T&D Company, Inc
1021 Main Campus Drive
Raleigh, North Carolina 27606

Abstract

With the advances in semi-conductor devices, adjustable speed drives (ASDs) have become more prevalent than ever before in industrial and commercial processes. Many facilities are installing ASDs to improve the efficiency of their processes and to increase the control of their processes. While the effects of ASDs on the power system are well known, many engineers and systems integrators are not aware of the effects that ASDs can have on the motor that is driven by the drive.

This paper describes the techniques used to measure, analyze, and simulate the problems associated with the use of PWM ASDs to drive induction motors. Measures to mitigate these problems are also discussed. The Electro-Magnetic Transients Program (EMTP) is used to simulate the phenomena, compare results against measurements, and evaluate mitigation techniques.

Introduction

In general, ac motor ASDs can be divided into two basic categories according to the working principle of the drives circuitry:

1. Phase controlled front-end rectifiers, output current source inverter (CSI)

2. Uncontrolled diode-bridge rectifier front-end, dc link, and voltage source inverter (VSI)

Until the late 1980's, the inverters of large drives were thyristor based with either forced-commutation or load-commutation. For CSI drives based on thyristor or GTO devices, the inverter switching frequency was limited to several hundred Hz. This switching frequency implies that these devices have relatively high commutation losses and need a relatively long commutation period. Consequently, motors supplied by CSI drives will have less chance of seeing fast-front voltages and, therefore, are not discussed in this paper.

Drives for most small and medium sized induction motors may utilize voltage source inverters (VSI) to provide variable frequency ac output. The common drive structure adopted by industry consists of an uncontrolled diode-bridge rectifier, dc link, and PWM VSI inverter as shown in Figure 1. The dc link for the VSI type drive is basically a ripple smoothing capacitor. The inverter output waveform is generated by a series of step-like functions. An ideal step-change in the output voltage is prevented by stray parameters of the circuit and commutation of switching devices from one phase to another. Steep-front waveform generation is one of the inherent characteristics of a high frequency operation voltage source inverter.

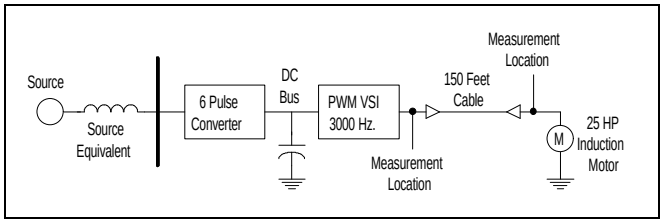

Figure 1: One Line Diagram Showing Power System and PWM Circuit.

The output of the PWM drive is of concern in this paper. Both frequency and magnitude of the output voltage are adjusted by controlling the inverter's operation. State of the art VSIs are based on IGBT technology. With IGBT devices, the inverter operates with a switching frequency ranging from tens of Hz to tens of thousands of Hz. Figure 2 illustrates the typical output voltage of a PWM drive. The switching frequency of the most commonly used PWM drives is in the range of 1000 Hz to 5000 Hz. The rise times of the pulses for IGBT VSIs can be on the order of 10 μs to 0.1 μs.

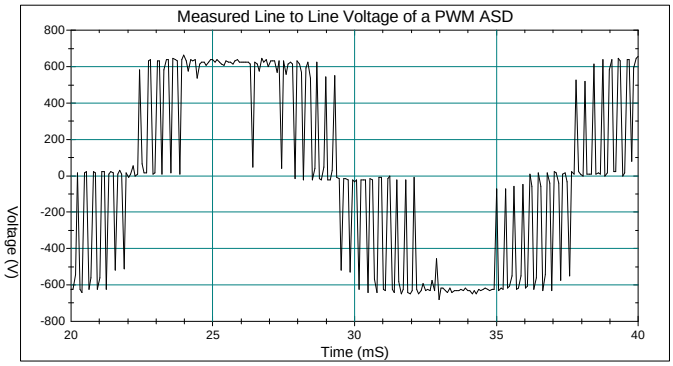

Figure 2: Measured Line-to-Line Output Voltage of a Typical PWM ASD.

The high switching frequency of IGBTs allow sophisticated PWM schemes to be implemented. One of the advantages of the high switching frequency inverter is the reduction of low order harmonics, which results in the reduction of the output filter requirements. However, this benefit can only be achieved under certain circuit conditions. Under some particular conditions, the fast changing voltage resulting from high frequency switching operation of IGBT VSIs can create severe insulation problems for an induction motor.

Machine insulation integrity is affected by the rate of change of voltage as well as the over voltage magnitude. A voltage with a high rate of change tends to be distributed along a motor's winding unevenly. This uneven distribution causes a significant over-stress across ending turns resulting in turn-to-turn insulation failure. In practice, it is common for the drive and the motor to be separated by long lengths of cable. Usually, the characteristic impedance of the motor can be ten to one-hundred times that of the characteristic impedance of the cable connecting the drive to the motor.

The most harmful effect of the PWM ASD output occurs when the connection cable is relatively long with respect to the wave front of an incidental voltage wave and when the ratio of characteristic impedance of the machine and the cable is high. In the worst case, an inverter output voltage pulse magnitude can be doubled at the induction motor terminals. Assuming that a voltage wave travels at a velocity of 250 feet per micro-second, an incident voltage wave with a front time of 0.3 micro-seconds is sufficient to create a voltage doubling at the open end of 75 feet of cable. Under this condition, motor windings experience a near 2.0 pu over voltage, if the maximum voltage seen at the inverter output terminal is 1.0 pu.

The reflection of an incident traveling voltage wave at the motor connection termination is determined by surge impedance ratio at the junction point. The incident voltage reflections under three extreme conditions are given below:

1. If the cable termination surge impedance is zero (e.g. a capacitor), the reflected wave at the end of the cable will be equal in magnitude but with a negative sign, resulting in a net zero transient.

2. If the cable is open at the end, the reflected voltage at the end of the cable will be equal in magnitude with the same sign, resulting in two times the magnitude of the incident voltage on the other side of the junction.

3. If the cable is terminated by an impedance that matches the characteristic impedance of the cable, the incident voltage will not be reflected, a refraction voltage equal to the incident voltage will result.

The characteristic (Equation 1) impedance of a small motor is usually higher than the low surge impedance of the cable. Therefore, when compared with the low surge impedance of cable, the motor connection looks like an open circuit to incident voltage waves.

$$Z_m = \sqrt{\frac{L}{C}} \qquad \textit{Equation 1}$$

Measurements

Figure 1 illustrates the one-line representation of the circuit that was used for the measurements. The ASD was a 25 hp PWM drive running a cooling fan motor. The ASD was housed in a steel shack in the middle of the desert approximately 100 to 150 feet away from the cooling fan. Using a 50 MHz digital storage oscilloscope, the voltage

pulses were measured at the output of the PWM VSI drive and at the motor terminals. The results are shown in Figure 3 and Figure 4, respectively. The measurement points are indicated on the one-line diagram in Figure 1.

Figure 3 illustrates a transition in one of the pulses at the output of the PWM voltage source inverter drive. Notice that when the voltage changes from zero to its full negative value, there is no over shoot or over voltage. At the motor terminals, however, the transition of one of the pulses at the motor terminals shows an over voltage of approximately 1.7 pu, as illustrated in Figure 4. This over voltage and ringing occurs at both the front and rear of each pulse. Depending on the operation pattern of the drive, similar transients may occur 20 to 100 times per 60 Hz cycle. As much as 85% of the peak transient voltage will be dropped across the first turn of the first coil of the motor phase winding.[1]

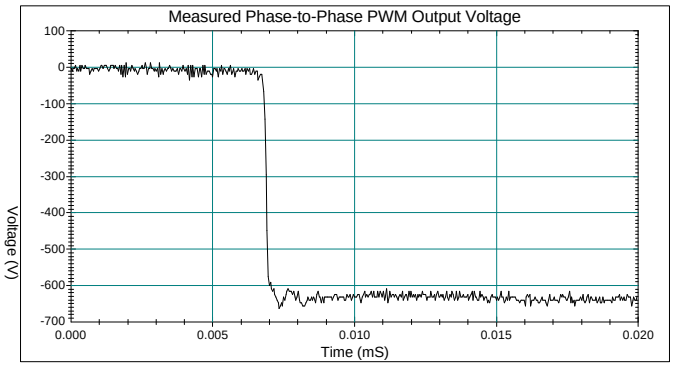

Figure 3: Measured Phase-to-Phase Voltage at PWM VSI Terminals.

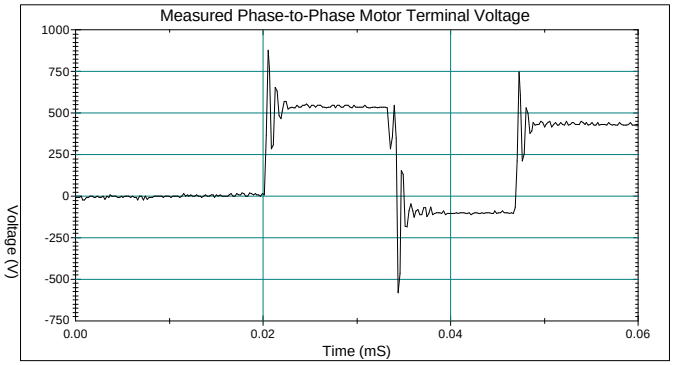

Figure 4: Measured Phase-to-Phase Voltage at Motor Terminals.

It is unlikely that the inter-turn insulation of the machine fails immediately at one surge impact. However, damaging effects to the machine winding insulation are accumulated over a period of time. It is very likely that dielectric partial discharging occurs in the ending region of the machine winding. This can greatly accelerate the dielectric material aging process. Consequently, the life of the machine insulation can be much shorter than normally expected. The worst case is when the partial discharging forms a fixed channel and eventually causes major insulation failure.

From the motor terminal voltage measurement, the characteristic impedance of this 25 hp motor was derived and expressed in terms of a surge impedance of the cable. Based on the expression relating the cable surge impedance, *Zc*, the machine characteristic impedance, *Zm*, and voltage refraction coefficient, *a*, the following equation can be obtained:

$$a = \frac{2 Z_m}{Z_c + Z_m} = 1.7 \text{ and } Zm = 5.67\ Zc \quad \text{Equation 2}$$

Usually, as machine rating increases, the equivalent winding capacitance increases and equivalent winding inductance decreases. Based on this reasonable assumption, the following remark is made that the discussed problem has the greatest chance of happening when an IGBT based VSI type of drive is used to supply a small machine through a relatively long cable. For large machines, this is less likely to occur due to the following:

- Large machines are more likely to be driven by a CSI type drive. Therefore, fast front voltage generation is not a concern. Motor terminal voltage is forced to change during a current switching. The voltage spikes are controlled by required ac filters.

- IGBTs are not able to be used at the present time in high power level applications because of device rating and economic considerations. Relatively low switching frequencies and relatively high switching losses associated with thyristor or GTO devices, and losses associated with the inverter auxiliary circuits, effectively prevent these inverters from generating fast rate of change voltages.

- Large machines tend to have relatively low characteristic impedance which helps to reduce terminal voltage doubling effect.

Model Development and Validation

The EMTP model for the system illustrated in Figure 1 was developed to simulate the behavior of the discussed drive-motor operation. Pre-developed EMTP data input modules (representing major circuit components in this simplified drive circuit) were used as building blocks to build the system model. The results of the simulations corresponding to the phenomena illustrated in Figures 3 and 4 are shown in Figures 5 and 6, respectively. The EMTP simulation results match the measurements well.

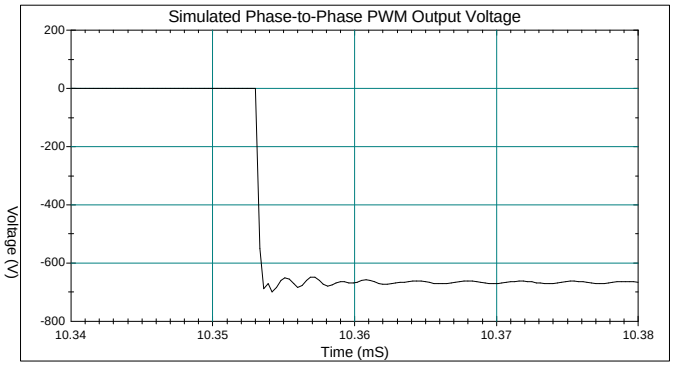

Figure 5: Simulated Phase-to-Phase Voltage at PWM Terminals.

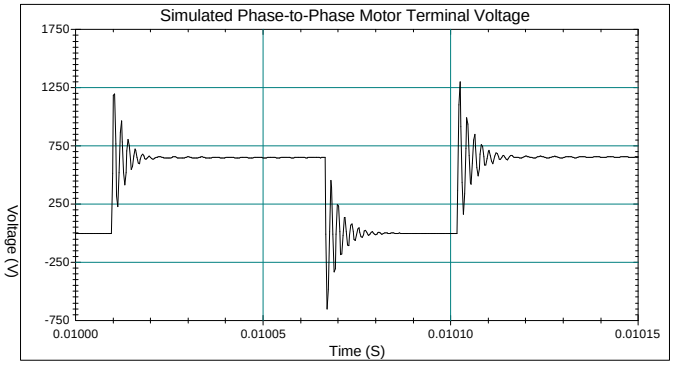

Figure 6: Simulated Phase-to-Phase Voltage at Motor Terminals.

Two cases were developed: one case to simulate and validate the system described in Figure 1, and a second case to develop graphs and tables to enable estimations of the overvoltages expected for various cable lengths and machine horsepower ratings. The induction motor was modeled by the surge impedance of the motor.

Table 1 shows the values of the surge impedance for various horsepower ratings of the induction machine. The characteristic impedance of the cable was approximately 50 ohms. The capacitor in the dc link was 5000 μF. The actual dc bus voltage simulated was 740 Volts dc (1.0 pu).

Table 1: Horsepower Ratings verses Surge Impedance Zm.

Motor HP	Surge Impedance
25	1500 Ω
50	750 Ω
100	375 Ω
200	188 Ω
400	94 Ω

The switching frequency for the remainder of the cases was reduced to 1200 Hz. Two sets of cases were developed. The first set of cases evaluated the effects of varying the cable length while keeping the horsepower of the machine constant and the second set of

cases evaluated the effects of varying the horsepower of the induction machine while the cable length remained constant. The results of these cases are shown in Figures 7 and 8 respectively.

Figure 7 illustrates that as the cable length is increased, the maximum overvoltage seen at the motor terminals increases. This is explained by the transmission line theory. Table 2 shows data obtained from a drive manufacturer concerning the critical cable lengths for different inverter topologies. The results of the simulations for IGBTs match the findings in Table 2.

Table 2: Findings of Drive Manufacturer.[5]

Inverter Technology	Critical Cable Length
IGBT	100 - 200 ft.
Bipolar	250 - 500 ft.
GTO	600 - 1000 ft.
SCR	600 - 1000 ft.

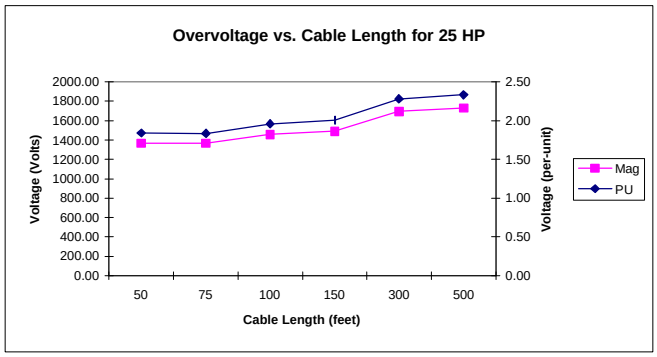

Figure 7: Maximum Overvoltage at Motor Terminals for Various Cable Lengths.

Since the overvoltage magnitude is related to the characteristic impedance of the cable versus the impedance of the motor windings, simulations were run to compare the overvoltage versus drive/motor size. For these simulations, cable length was kept constant while the HP rating of the motor was varied. Figure 8 shows the results of these simulations.

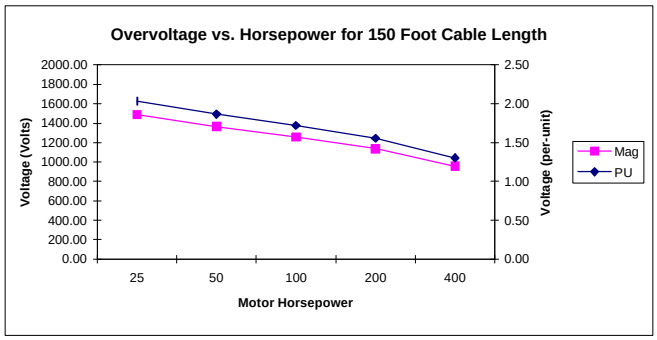

Figure 8: Maximum Overvoltage at Motor Terminals for Various HP Ratings.

The results in Figure 8 show that as the motor horsepower was increased, the overvoltage at the motor terminals decreased. This is explained by the rules of incident voltage reflections. As the motor horsepower is increased, the surge impedance of the motor decreases (see Table 1) and more closely matches the characteristic impedance of the cable. For smaller horsepower motors (e.g. 25 HP) the surge impedance of the motor can be 30 times greater than the characteristic impedance of the cable, essentially an open circuit. While for a large horsepower motor (e.g. 400 HP) the surge impedance of the motor is approximately twice the cable impedance, resulting in a much lower reflected voltage.

For all the simulations, the front time step-like voltage pulse was assumed to be 0.1 micro-seconds. The voltage magnitude of over 2.0 pu as given in Figure 7, can be explained by the following.

If the dc bus voltage is selected as the voltage per unit base, the inverter terminal voltage can be greater than 1.0 pu. This has been shown by the measurement waveform presented in Figure 3. Due to some local oscillation, the inverter terminal voltage can reach 1.1 to 1.3 pu.

When the connecting cable becomes longer, the circuit capacitance increases rapidly. However, for this circuit, the equivalent loop inductance and resistance are dominated by the motor. With an increased cable length and the same motor, the natural frequency and damping factor of the circuit loop both decrease. Consequently, the transient voltage oscillation after each IGBT switch lasts longer. When switching action takes place consecutively, and if the second transient is initiated before the previous oscillation is completely damped out, the second switching pulse has an initial component greater than 1.0 pu (Figure 9), resulting in a motor terminal transient greater than 2.0 pu.

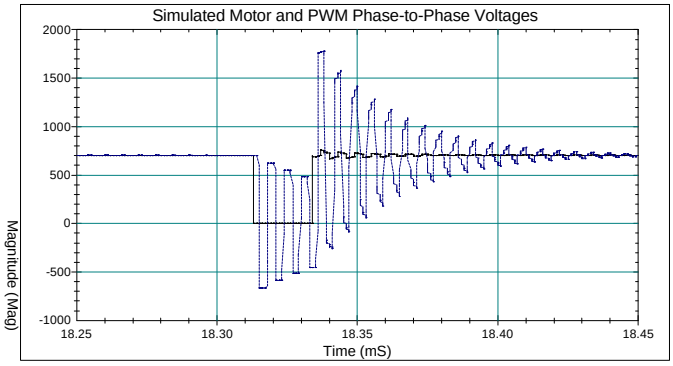

Figure 9: Simulated Motor (dashed) and PWM (solid) Phase-to-Phase Voltages Illustrating Greater than 2.0 pu Overvoltage.

Evaluation of Mitigation Methods

There are many potential mitigation techniques which might be employed to solve the over voltage problem at the motor terminals. With the proven EMTP simulation model, effectiveness of two promising solution methods were explored:

- Install a line choke, in series with the connection cable, on the output of the PWM drive.
- Install a capacitor, in parallel with the motor, at the motor terminals.

To evaluate the choke solution, a 5% (on the base of the 25 hp motor) inductor was inserted between the drive output and the connecting cable at the drive output terminals. The resulting phase-to-phase voltages at the drive output terminals and at the motor terminals are plotted together in Figure 10. This ac output choke failed to control motor terminal over voltage as illustrated in Figure 10.

The choke inductance did help to reduce the rate of change of the voltage seen by the motor. However, the choke created an extra circuit mesh which formed its current loop through the inverter source, choke inductance and cable equivalent capacitance. If the source impedance can be ignored (which is very likely to be the case for the drive with a sufficient dc capacitance and low on-state real and reactive power losses) the natural frequency of this loop can be easily estimated using the choke inductance and cable positive sequence equivalent capacitance. Very light losses are associated with this high frequency oscillation loop. Therefore, every time an IGBT is switched, the step voltage applied to the loop excites the natural oscillation with very light damping. Because the inverter switching may occur at any point on this natural oscillation voltage waveform, the initial conditions resulting from immediate previous switching is added to the next switching transient. Consequently, the motor experiences an over voltage exceeding twice of what the inverter generated. Introducing enough damping in this added loop should be able to make this solution effective. However, simple calculation shows that it is impractical because of excessive overall circuit losses.

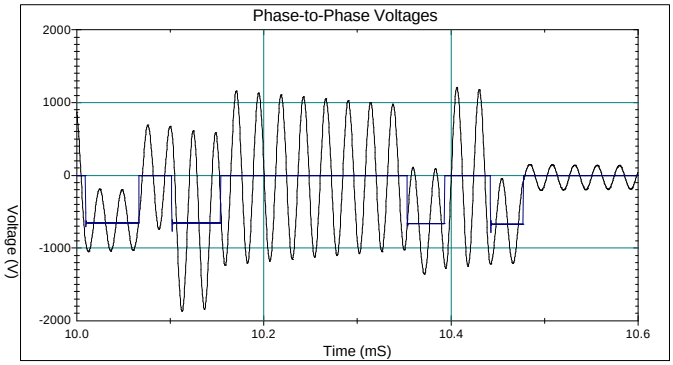

Figure 10: Phase-to-Phase Voltage at Drive Output and Motor Terminal.

The idea of installing capacitance at the motor terminal is initially drawn from the concept of matching the cable surge impedance with the characteristic impedance seen at the

motor terminals. However, a precise matching of the impedance may require an amount of capacitance which is undesired for overall system consideration. Therefore, a compromise solution is to add some amount of capacitance to reduce the motor terminal characteristic impedance, and to introduce the proper level of damping to control the voltage overshoot. Based on this concept, three basic damping circuits can be used:

- An over damped circuit
- A critically damped circuit
- An under damped circuit

Each circuit includes a resistance in series with a capacitor. This series combination will be in parallel with the motor's windings. The EMTP simulations showed that the best results were obtained when a critically damped circuit was employed at a properly selected resonant frequency. This method assures that the pulse at the end of the cable more closely matches the pulse at the beginning of the cable.

Knowing the switching frequency of the PWM drive was 3000 Hz and based on practical experience, it was decided that a good resonant frequency for the damping circuit would be five times the switching frequency or 15,000 Hz. Using the inductance of the cable (0.027 mH for 150 ft. of # 8 AWG) the value of the capacitance was calculated to be 4.2 μF and the damping resistance was selected to be 5.5 ohms. This circuit's damping resistance was calculated based on 15,000 Hz.

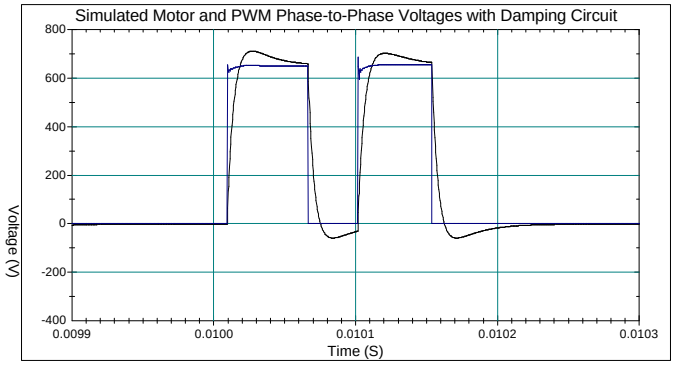

Figure 11: Simulated Phase-to-Phase Voltage at PWM Output and Motor Terminals with Damping Circuit Installed.

Figure 11 illustrates the effect that the introduced RC circuit has on the voltage at the motor terminals. The negligible over shoot in the voltage waveform illustrates that the circuit is slightly under damped. However, this approach does seem to have some merit. The high voltage reflection at the motor terminals is well under control and the over voltage is less than 1.2 pu. But, even more importantly, the steep front of the voltage pulse has been greatly reduced.

Design Related Issues

The way in which the motors are designed and wound plays an important role in the integrity of the motor performance when used with PWM drives. Factors like winding type and insulation methods need to be considered.

In a motor wound randomly, for instance, the first and last turn of each phase coil may be positioned next to each other physically (see Figure 12). This positioning of the first and last turn of each coil will increase the likelihood that the excess voltage will damage the motor windings. On the other hand, with concentric windings, each layer of the coil is laid on top of the previous layer. This ensures that the start and finish turns of each coil are separated.[5]

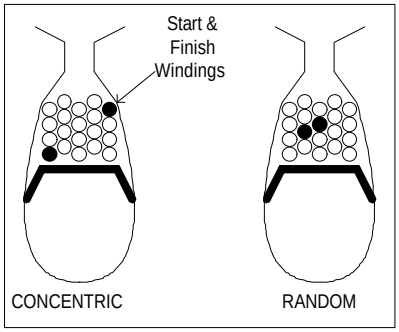

Figure 12: Motor Winding Coil Placement.

The insulation used in the slots and between phase coils also plays a part in the motor's integrity. In order to reduce costs, some manufacturers have reduced, or even omitted, the phase and slot papers (Figure 13). Motors are becoming smaller and more energy efficient, thus compressing the same number of turns into a smaller physical space. Slot and phase papers and top sticks are vital to increasing the motor's withstand capability to fast-front transients and prevent damage to the coils during construction.

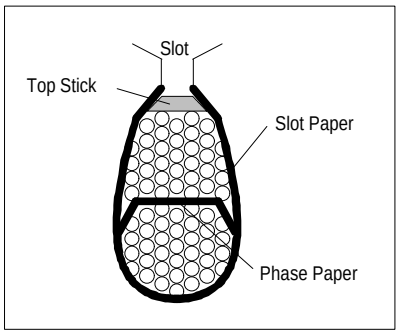

Figure 13: Motor Slot Insulation Diagram.

The best case for insulation is where slot paper, phase paper, top sticks, and coil insulation (insulation between coils on each end of the stator) are used. If at all possible, extra insulation should be used on the start and end turns of each winding.

Most slot paper is manufactured with alternating layers of paper (Daycron, silicon glass, etc.) and mylar. Below are typical grades for Daycron-Mylar paper.

- 3-5-3: 3 mil paper, 3 mil mylar, 3 mil paper
- 5-5-5: 5 mil paper, 5 mil mylar, 5 mil paper

The dielectric strengths for each of the papers listed above is 12,000 Volts and 12,500 Volts respectively. Slot paper is typically used for both the slot and phase papers while the top sticks are either made from wood or paper.

ASD manufacturers are now working with motor manufacturers to match drive duty motors to their drives. The ASD and motor come as a complete package. In fact, some motor manufacturers will not honor warranties for motors that are driven by ASDs and, in the case of new installations, require that the drive and motor be purchased as a package. The induction motors are designed to withstand the severe duties imposed on them by the high switching frequencies of the PWM drives.

Conclusions

When supplying squirrel cage induction motors from a PWM drive, care should be taken in the length of the cable feeding the motor. The authors have seen cases where a cable length as short as fifty feet caused a transients problem at the motor terminals. Conversely, there have been cases where the cable length was over 200 feet without adverse effects. If the problem is detected, an effective solution is to parallel an RC branch right at the motor terminals. Parameter selection for this RC branch are based on the drive circuit information and should be determined on case-by-case basis.

References

[1] Persson, Erik, “Transient Effects in Application of PWM Inverters to Induction Motors”, PID-91-28, IEEE Industry Applications Society, 1991 Pulp and Paper Industry Conference, Montreal, Canada, June 3-7, 1991.

[2] Daugherty, Roger H., Carl H. Wennerstrom, “Need for Industry Standards for ac Induction Motors Intended for Use with Adjustable-Frequency Controllers”, PID-91-05, IEEE Petroleum and Chemical Industry Technical Conference, Houston, TX, Sept. 10-12, 1990.

[3] Mecker, Steven L., “Consideration in Derating Induction Motors for Applications on Variable Frequency Drives”, CH3142-7/92/0000-0191, IEEE 1992.

[4] Melhorn, Christopher J., Le Tang, “Effects of PWM ASDs on Standard Squirrel Cage Induction Motors”, 1994 PCIM Conference Proceedings, Dallas, Texas, September 1994, pp. 356-364.

[5] Allen-Bradley Bulletin 1336 Plus IGBT Technology, Application Note #114, May, 13, 1994.

[6] Bonnet, Austin, “Analysis of AC Induction Motor Transients Caused by PWM Inverters”, 1993 PQA Conference Record, San Diego, CA, November, 1993, pp. 4-3:1 - 4-3:14.

Biographies

Christopher J. Melhorn (SM ‘86, M ‘90) was born in Portsmouth, VA on 06/23/64. He received an AS degree in Engineering from York College of Pennsylvania (1986) and a BS degree in Electrical Engineering Technology from Pennsylvania State University (1989).

Chris has been employed with Electrotek Concepts, Inc. since 1990. His experience at Electrotek includes working with EPRI and utilities on case studies involving power quality issues. He was also extensively involved in the EPRI DPQ project site selection phase. Chris is presently involved in developing new software for the power systems engineering environment and working to increase Electrotek's industrial based clientele.

Le Tang (M ’90), was born in Beijing, China. He received his BS degree in Electrical Engineering in 1982 from Xi'an Jiaotong University, Xi'an, China, his MEng. and Ph.D in Electric Power Engineering from Rensselaer Polytechnic Institute in 1985 and 1988 respectively. Dr. Tang conducts harmonics, transients and other power quality related analyses and studies. He is actively involved in renewable energy development and application, including wind electric power generation and its interface with electric utility systems.

A REFLECTION ON THE SUBJECT OF CONVERTERS INTERNAL HARMONIC IMPEDANCE

*Olívio C. N. Souto, MSc - *José Carlos Oliveira, PhD - *Aloísio de Oliveira, Dr
**Paulo F. Ribeiro, PhD

*Federal University of Uberlandia
Department of Electrical Engineering
Phone-Fax: 034 - 236 - 5099
38400-902 - Uberlandia - MG - Brazil

**Babcok & Wilcox
Product Development Department
Lynchburg, VA 24505
USA

ABSTRACT

Traditionally, harmonic studies use the converters modelled by ideal equivalent harmonic current sources for specific frequencies. Although this approach has been proved to be adequate for the majority of harmonic flow studies, the same may not happen for other applications. Thus, this paper aims to discuss an alternative model which proposes a more complete converter's Norton equivalent circuit for individual frequencies. This uses a combination of the harmonic current source produced by the converter and its internal harmonic impedance. The method is useful for studying subjects such as harmonic cancellation strategies.

INTRODUCTION

The widespread application of power electronics and others is increasing the number of electrical loads which distort the current and the voltage supplied by the ac line. The harmonic voltage and current in the power system can result in overloaded phase and neutral conductors, overheating of transformers and motors, interference with the operation of sensitive electronic equipment, etc. As part of the network study, it is necessary to simulate harmonic power flow to investigate the harmonic current and voltage levels in the system. Many authors and software packages treat the non linear loads by means of the ideal equivalent harmonic current sources [1], [2]. Although this approach is practical because of its simplicity and rapidity, it might be inaccurate for some applications. According to [3], the harmonic currents produced by converter loads are not constant as the operating conditions changes. In addition, harmonic currents absorbed or injected by a non linear load depend on the voltage applied to the non linear load. Ref. [4] proposes an alternative way to represent a non linear load by a "crossed-frequency" harmonic admittance matrix. In order to contribute towards this direction, this paper is concerned with the investigation of the converter harmonic current generation behaviour under distorted voltage supply. An equivalent circuit using Norton approach is then proposed for a six pulse converter, and a fully discussion of the converter internal harmonic impedance is also given. A time-domain simulation using the well known PSPICE is used to verify the proposed model performance.

THE EFFECT OF DISTORTED VOLTAGE ON HARMONIC GENERATION

To illustrate the behaviour of a non linear load under distorted supply voltage, a typical installation consisting of a six pulse rectifier is considered under different supply conditions. The system simulated is shown in Fig. 1.

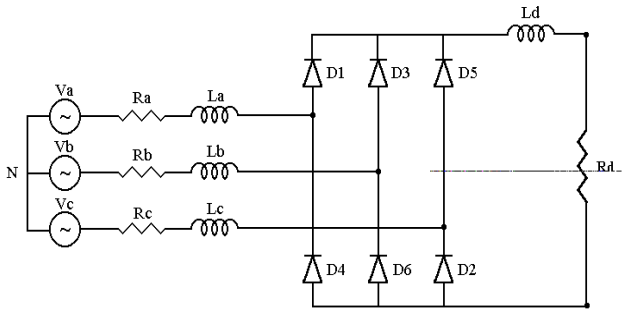

Fig. 1 - Six-Pulse converter

The AC line current waveforms under two different voltage supply are given in Fig. 2. The first is related to a purely sinusoidal voltage supply and the second with 15% of fifth harmonic voltage superimposed upon the fundamental value.

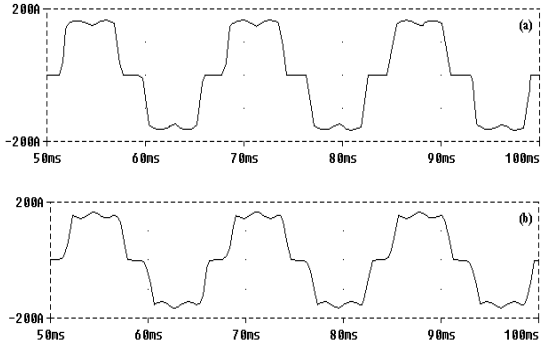

Fig. 2 - Line current supplying the converter.
(a) - Purely sinusoidal vaoltage condition
(b) - Distorted voltage with 15% of fifth harmonic

The corresponding harmonic spectrum for the above currents are shown in Fig. 3, in which it can be seen that the harmonic currents are substantially modified in magnitude although the orders are still the same.

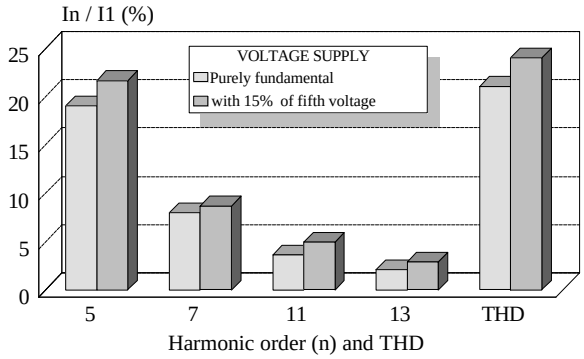

Fig. 3 - Line currents harmonic spectrum.

By changing the magnitude of the individual fifth and seventh harmonic voltage superimposed upon the fundamental value, a more comprehensive set of results is obtained. Figures 4, 5, 6 and 7 illustrate the harmonic currents produced by the converter with different levels of fifth, seventh, eleventh and thirteenth voltage distortion with specific phase-angles.

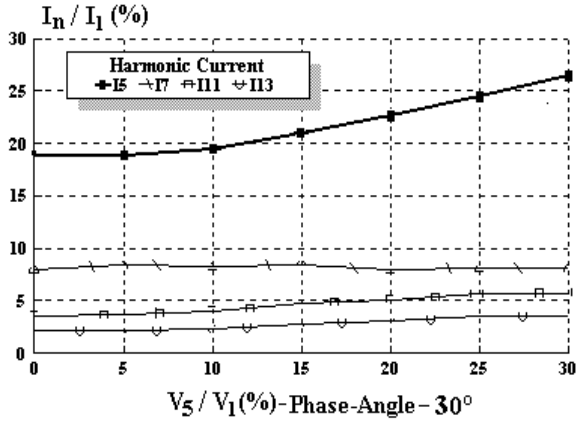

Fig. 4 - Harmonic current distortion vs. harmonic voltage with phase angle = 30°.

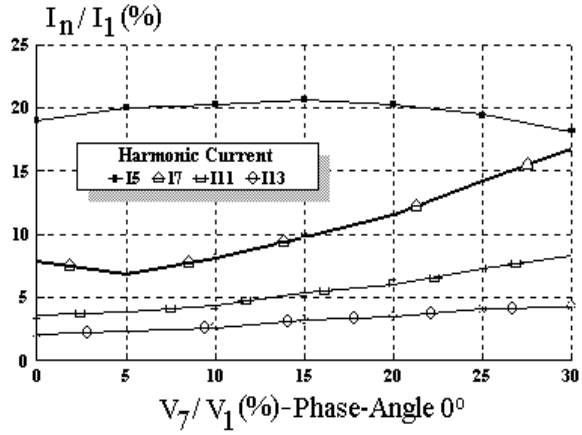

Fig. 5 - Harmonic current distortion vs. harmonic voltage with phase angle = 0°.

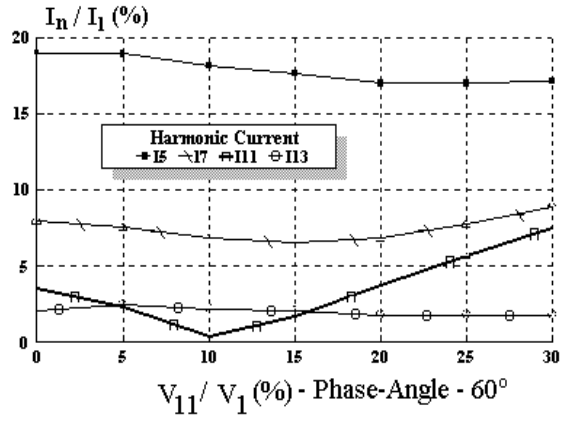

Fig. 6 - Harmonic current distortion vs. harmonic voltage with phase-angle = 60^0

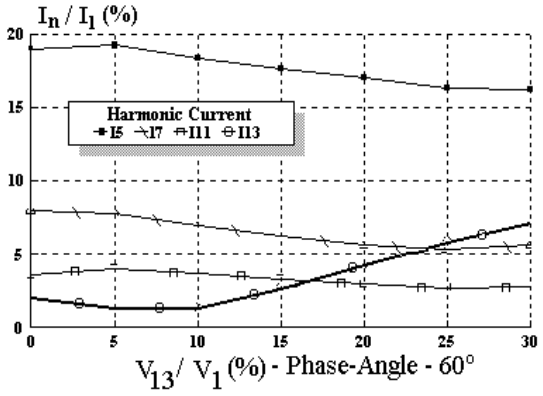

Fig. 7 - Harmonic current distortion vs. harmonic voltage with phase-angle = 60^0

It can be seen that the harmonic currents injected into the system by the converter are not constant when the voltage supply is distorted, so the classical model which neglects the new supply voltage waveform is not appropriate. In addition to this, the results indicate that the harmonic current orders which are more affected are those with the same frequency as the voltage distortion. The others are not substantially modified. This implies that, there is a degree of independence between harmonic voltage distortion and harmonic current of different order.

PHYSICAL INTERPRETATION OF THE FREQUENCY DOMAIN EQUIVALENT CIRCUIT

In general, for harmonic study purposes, a given non linear load can be described by the well known frequency domain technique. This uses a harmonic current source in parallel with an internal harmonic impedance. Because the shunt impedance associated with the non linear load is quite large in comparison with the internal impedance of the supply power system, many authors adopt this impedance as being infinite. Although this assumption is a common practice and useful for many applications, this may not be true

for other studies. As a matter of fact, the previous results suggest that a more realistic model, such as the frequency domain Norton equivalent circuit given in Fig. 8, should be used.

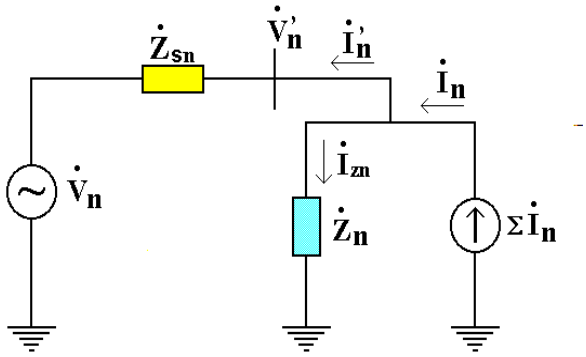

Fig. 8 - Norton equivalent circuit for a non linear load and the supply system.

In Fig. 8:

- $\dot{Z}_{sn}$ - Supply system harmonic impedance
- $\dot{Z}_{n}$ - Non-linear load internal harmonic impedance
- $\dot{I}_{n}$ - Harmonic current generated by the non-linear load
- $\dot{I}_{Zn}$ - Harmonic current flowing through the internal impedance
- $\dot{I}'_{n}$ - Harmonic current injected into the supply.
- $\dot{V}'_{n}$ - Harmonic voltage at non-linear load terminals.
- $\dot{V}_{n}$ - Supply system harmonic voltage

From Fig. 8 the following expressions can be obtained:

$$\dot{I}'_n = \dot{I}_n + \dot{I}_{Z_n} \qquad (1)$$

$$\dot{I}_{Z_n} = \frac{\dot{V}'_n}{\dot{Z}_n} \qquad (2)$$

Through the equivalent circuit it can be seen that by modifying the harmonic voltage at the non linear load terminals, then the corresponding harmonic currents $\dot{I}'_n$ and I_{zn} will be changed. In fact, the new currents will be a combination of the internal harmonic generation and that injected by the harmonic voltage applied.

When the supplied voltage is purely sinusoidal or close to this, the harmonic currents produced by the converters find an electrical path which consists of a parallel combination of Z_{Sn} and Z_n. As Z_n is greater than Z_{Sn}, the majority of I_n flows towards the supply. However, when a voltage distortion appears at the converter terminal, this forces a

corresponding harmonic component of current to flow into Z_n. The combination of the previous harmonic current injected into the supply and that injected into the internal impedance will modify the total current flowing from converter terminals. Equations 1 and 2 allow for these calculations.

A GENERAL FORMULATION

Although the previous analysis does not take into account the harmonic coupling between different voltage and current harmonic frequencies, a more general way for representing the relationship between the internal harmonic impedance and corresponding terminal voltage and current can be expressed by the matrix formulation bellow:

$$\left[\dot{V}_{Z_i}\right] = \left|\dot{Z}_{ij}\right| \left[\dot{I}_{Z_i}\right] \qquad (4)$$

where:

$\left[\dot{V}_{Z_i}\right]$ - Harmonic voltage distortion of order "i"

$\left|\dot{Z}_{ij}\right|$ - Non-linear load internal harmonic impedance matrix

$\left[\dot{I}_{Z_i}\right]$ - Harmonic current of order "i" through the internal harmonic impedance.

The above formulation applied to a six pulse converter operating under ideal conditions leads to:

$$\begin{bmatrix} \dot{V}_{Z_5} \\ \dot{V}_{Z_7} \\ \dot{V}_{Z_{11}} \\ \dot{V}_{Z_{13}} \end{bmatrix} = \begin{bmatrix} \dot{Z}_{5,5} & \dot{Z}_{5,7} & \dot{Z}_{5,11} & \dot{Z}_{5,13} \\ \dot{Z}_{7,5} & \dot{Z}_{7,7} & \dot{Z}_{7,11} & \dot{Z}_{7,13} \\ \dot{Z}_{11,5} & \dot{Z}_{11,7} & \dot{Z}_{11,11} & \dot{Z}_{11,13} \\ \dot{Z}_{13,5} & \dot{Z}_{13,7} & \dot{Z}_{13,11} & \dot{Z}_{13,13} \end{bmatrix} \times \begin{bmatrix} \dot{I}_{Z_5} \\ \dot{I}_{Z_7} \\ \dot{I}_{Z_{11}} \\ \dot{I}_{Z_{13}} \end{bmatrix} \qquad (5)$$

Although the term "impedance" should not be used to relate different voltage and current frequencies, the general "harmonic impedance $Z_{i,j}$" has only the meaning of providing a coupling factor between harmonic current and voltage of different order. On the other hand, the "impedance $Z_{i,i}$" expresses the relationship between harmonic voltage and current of same order, therefore, the term could be properly used.

If the coupling of different frequencies can be neglected, then the following expression applies:

$$\dot{V}_{Z_i} = \dot{Z}_{i,i} \times \dot{I}_{Z_i} \qquad (6)$$

AN EXAMPLE OF INTERNAL HARMONIC IMPEDANCE CALCULATION

To verify the theory, a time-domain analysis was carried out using the software package PSPICE to simulate the circuit given in Fig. 1. The simulation was carried out in order to calculate the harmonic currents produced by the converter under different voltage distortion conditions. Using the previous formulation, it was then possible to evaluate what has been called by "non linear load harmonic internal impedance". Both "coupling impedance" and "proper impedance" are given.

By applying a harmonic distortion of order 5 upon the fundamental voltage, Figures 9, 10, 11 and 12 give, respectively, the impedances $Z_{5,5}$, $Z_{7,5}$, $Z_{11,5}$ and $Z_{13,5}$. The results indicate that the "proper impedance" is smaller than the "coupling impedance". Similar conclusions could be derived from other orders. The effect of the voltage distortion phase-angle can be also seen.

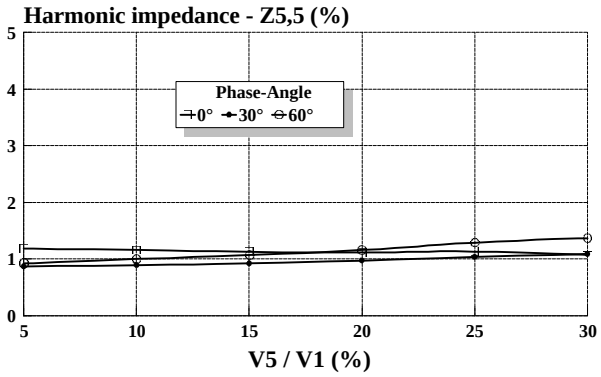

Fig. 9 - Converter harmonic impedance $Z_{5,5}$.

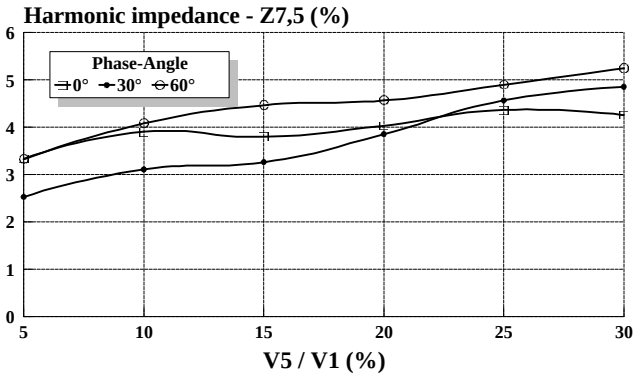

Fig. 10 - Converter harmonic impedance $Z_{7,5}$

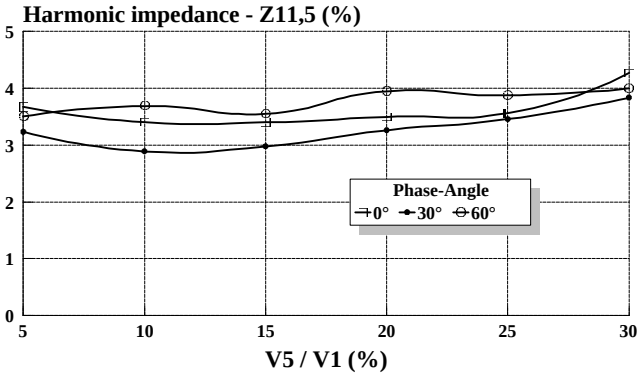

Fig. 11 - Converter harmonic impedance $Z_{11,5}$

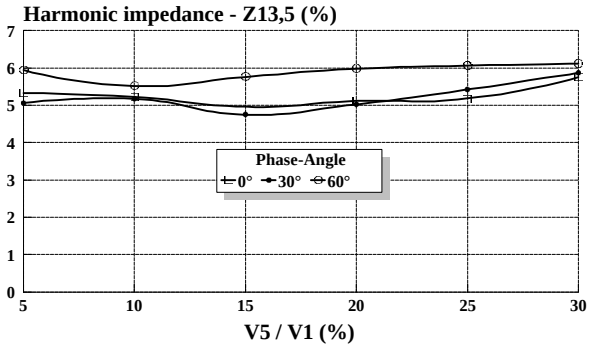

Fig. 12 - Converter harmonic impedance $Z_{13,5}$

A COMPARATIVE TIME AND FREQUENCY DOMAIN HARMONIC CALCULATION

By modelling the six pulse converter into the PSPICE program under different distorted voltage and using the previous formulation, it is possible to compare the results achieved using time and the proposed frequency domain techniques.

Tables I and II give the final results associated to specific voltage distortion. The errors are relatively small and the good agreement between the harmonic currents calculated with both methods has shown that the frequency domain proposed model is a reasonable tool to deal with the subject.

VOLTAGE SUPPLY (Phase A) Fundamental Component : $V_{1\,max.}$ = 310 V∠0° [V] (100%) Fifth harmonic distortion : $V_{5\,max.}$ = 55,8 ∠45° [V] (18%)					
HARMONIC ORDER	LINE CURRENT (Phase A) – [A]				ERROR (%)
	SIMULATION		CALCULATION		
	MAGNITUDE	PHASE-ANGLE	MAGNITUDE	PHASE-ANGLE	
5	24.30	47.78	24.56	49.18	1.07
7	7.99	41.39	8.12	39.72	1.64
11	5.46	88.18	5.39	93.68	1.28
13	3.09	55.74	2.87	54.8	7.12

Table I-18% of fifth voltage distortion.

VOLTAGE SUPPLY (Phase A) Fundamental Component : $V_{1\,max.}$ = 310 V∠0° [V] (100%) Fifth harmonic distortion : $V_{5\,max.}$ = 37,2∠67° [V] (12%) Seventh harmonic distortion : $V_{7\,max.}$ = 9,3 ∠12° (3%)					
HARMONIC ORDER	LINE CURRENT (Phase A) – [A]				ERROR (%)
	SIMULATION		CALCULATION		
	MAGNITUDE	PHASE-ANGLE	MAGNITUDE	PHASE-ANGLE	
5	23.89	64.33	23.65	66.03	1.05
7	7.66	77.64	7.76	79.90	1.31
11	5.62	109.10	5.16	112.96	8.18
13	3.24	78.9	3.06	80.92	5.55

Table II -12% of fifth and 3% of seventh voltage distortion.

CONCLUSIONS

A comprehensive way to model non linear loads using frequency domain technique was given in this paper. A particular application using a typical six-pulse converter into the well known PSPICE simulator was performed in order to illustrate the theory and to provide results to compare time-domain with the proposed frequency domain final harmonic currents. The new approach allows studying the harmonic behaviour of non linear loads under distorted voltage supply. The results were quite promising in showing that, the use of a more complete frequency domain equivalent circuit, may be of great importance when non ideal supply conditions are considered. Besides the frequency domain technique, a fully discussion on the subject of “proper internal impedance” and “coupling internal impedance” was given. It was shown that the “proper impedance” has a more significative effect on the non linear load performance, when harmonic current calculation is considered. Although the results were promising, it must be emphasised that the subject deserves further investigations concerning different type of non linear loads, as well as laboratory experiments.

REFERENCES

[1] W.E.Kimbark, “DirectCurrentTransmission“, Vol.1, Wiley Interscience, John Wiley & Sons, New York, NY, 1971.

[2] J. Arrilaga, D.A. Bradley, and P.S. Bodger, “Power System Harmonics“, John Wiley & Sons, 1985, New York, NY, 1985.

[3] M. Taleb, and T. H. Ortmeyer, “Examination of the Current Injection Technique”, Proceedings of IEEE ICHIPS IV, 1991, Hungary.

[4] M. Fauri, and P. Ribeiro, “A Novel Approach to Non Linear Load Modelling”, Proceedings of IEEE ICHIPS VI, Bologna, Sep. 21-23, 1994.